

# Highly Efficient (R-X-R)-Type Carbamates as Molecular Transporters for Cellular Delivery

Kiran M. Patil,<sup>†,§</sup> Rangeetha J. Naik,<sup>‡,§</sup> Rajpal,<sup>‡</sup> Moneesha Fernandes,<sup>†</sup> Munia Ganguli,<sup>\*,‡</sup> and Vijayanti A. Kumar<sup>\*,†</sup>

<sup>†</sup>Organic Chemistry Division, National Chemical Laboratory, Dr. Homi Bhabha Road, Pune 411 008, India

<sup>‡</sup>Lab No. 203, Institute of Genomics and Integrative Biology, Mall Road, Delhi 110 007, India

## Supporting Information

**ABSTRACT:** The (R-X-R) motif-containing arginine-rich peptides are among the most effective cell-penetrating peptides. The replacement of amide linkages in the (R-X-R) motif by carbamate linkages as in (r-ahx-r)<sub>4</sub> or (r-ahx-r-r-apr-r)<sub>2</sub> increases the efficacy of such oligomers several-fold. Internalization of these oligomers in mammalian cell lines occurs by an energy-independent process. These oligomers show efficient delivery of biologically active plasmid DNA into CHO-K1 cells.

Cell-penetrating peptides (CPPs) have proved very useful as carriers for the intracellular delivery of several types of small molecular drugs as well as of peptide/oligonucleotide cargos for therapeutic applications. A significant number of CPPs are cationic in nature and contain at least six amino acids such as lysine or arginine which are positively charged at physiological pH. The repertoire of naturally derived CPPs such as Tat-peptide,<sup>1</sup> penetratin,<sup>2</sup> and pAntp<sup>3</sup> was later augmented by synthetic homopolymers of cationic  $\alpha$ -amino acids.<sup>4</sup> It was demonstrated that the guanidine headgroup of arginine in polyarginine peptides was the critical component for this efficiency.<sup>4,5</sup>

The arginines separated by  $\omega$ -amino acids (-X-) with variable chain lengths as in the (R-X-R) peptide motif were shown to be far better than the natural  $\alpha$ -amino acid-containing peptides,<sup>6</sup> probably due to their amphipathic nature. The arginine peptides interspersed with  $\epsilon$ -aminohexanoic acid (Ahx) (Figure 1) and  $\gamma$ -aminopropionic acid (Apr) were found to be among the most effective synthetic CPPs for highly efficient cargo transportation.<sup>7,8</sup> The mechanism of uptake of CPPs is still under debate, and it is postulated that it could be operating in multiple modes.<sup>9</sup> The (R-X-R)-type of peptides were found to be comparatively more stable to peptidases than the natural  $\alpha$ -

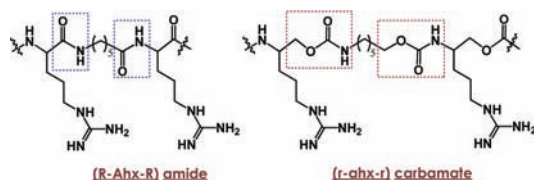


**Figure 1.** Representation of (R-Ahx-R) amide- and carbamate-linked oligomers chemically illustrating their backbone differences.

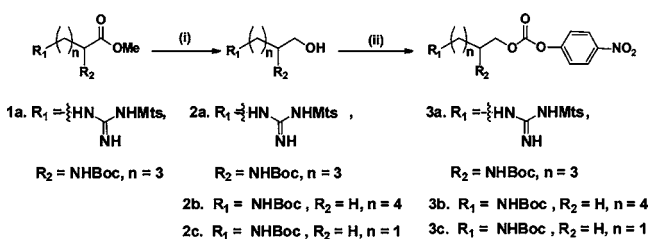
amino acid-containing peptides.<sup>10</sup> The peptide linkages at arginine sites were still amenable to cleavage for the (R-X-R)<sub>4</sub> peptides and caused toxicity.<sup>11</sup> Peptidomimetics such as peptoids,<sup>12</sup> oligoureas,<sup>13</sup> oligocarbonates,<sup>14</sup> and oligocarbamates<sup>15</sup> as transporters have been explored with an aim to increase the stability of the oligomers *in vivo*. Among the carbamate analogues, the oligoarginine sequences were synthesized and were found to have enhanced uptake properties.<sup>15</sup>

In this Communication, we report the design, synthesis, and uptake properties of carbamate-linked (r-x-r)-motif oligomers based on their (R-X-R)-type amide-linked counterpart. It was envisaged that the (r-x-r)-motif would exhibit synergistic properties when carbamate linker is used in tandem with appropriate spacer (-x-) for optimizing the interaction of two consecutive guanidine groups as in R-X-R (X = Ahx/Apr) with the cell membrane, leading to favorable uptake. The carbamate linkage adds O-CH<sub>2</sub> to the amide NH-CO (Figure 1), thus adding flexibility and hydrophobicity and reducing the possibility of hydrogen-bonded secondary structures.<sup>16</sup> This would probably leave the oligomers more amenable for adopting structural features better suited to interact with lipid membranes. Amino-hexanol (ahx) and aminopropanol (apr) linkers were used to separate selected adjacent guanidine functionalities and to optimize the effect of chain lengths on guanidinium display.

The carboxyfluorescein (CF)-tagged (R-Ahx-R)<sub>4</sub>\_amide\_CF (I) and unlabeled oligomer (R-Ahx-R)<sub>4</sub>\_amide\_Phe (IV) were synthesized employing standard Boc chemistry and used as controls to compare the cell uptake and cargo delivery capability of designed oligocarbamates (Table 1). The carbonate monomers for the synthesis of oligocarbamates were synthesized according to Scheme 1. The ester function in *N* $\alpha$ -Boc-L-Arg(Mts)-methyl ester **1a** was reduced to yield the corresponding alcohol **2a**. The hydroxyl groups in **2a**, *N*-Boc-amino-hexanol **2b**, and *N*-Boc-aminopropanol **2c** were each activated as their *p*-nitrophenyl carbonates by treating with *p*-nitrophenyl chloroformate in pyridine and dichloromethane to get the *N*-Boc-protected monomers **3a**, **3b**, and **3c**, respectively, for solid-phase carbamate synthesis. The oligocarbamates (r-ahx-r)<sub>4</sub>\_carbamate\_CF (II), (r-ahx-r-r-apr-r)<sub>2</sub>\_carbamate\_CF (III), and (r-ahx-r)<sub>4</sub>\_carbamate\_Phe (V) (Table 1) were

**Received:** October 25, 2011

**Published:** April 11, 2012

Scheme 1. Synthesis of Carbamate Monomers for Oligocarbamate Synthesis<sup>a</sup>

<sup>a</sup>Reagents and conditions: (i)  $\text{NaBH}_4\text{:LiCl}$  (1:1) (2.5 equiv), THF:EtOH (3:4) (2a, 89%); (ii) *p*-nitrophenyl chloroformate (1.2 equiv), dry pyridine (2.5 equiv),  $\text{CH}_2\text{Cl}_2$  (3a, 75%; 3b, 82%; 3c, 86%).

Table 1. MALDI-TOF Analysis of the Oligomers<sup>a</sup>

oligomer	MALDI-TOF mass	
	calcd	obsd
(R-Ahx-R) <sub>4</sub> _amide_CF (I)	2076.21	2077.35
(r-ahx-r) <sub>4</sub> _carbamate_CF (II)	2406.33	2408.40
(r-ahx-r-r-apr-r) <sub>2</sub> _carbamate_CF (III)	2322.24	2324.81
(R-Ahx-R) <sub>4</sub> _amide_Phe (IV)	1907.25	1907.33
(r-ahx-r) <sub>4</sub> _carbamate_Phe (V)	2237.36	2238.33
r <sub>8</sub> _carbamate_CF <sup>15</sup> (VI)	1833.95	1834.49
r <sub>8</sub> _carbamate_Phe (VII)	1664.98	1666.71

<sup>a</sup>R and Ahx denote amino acid residues; the lowercase r, ahx, and apr denote amino alcohol residues; CF denotes carboxyfluorescein. CF or Phe is at the N-terminus of oligomers.

synthesized manually on solid phase (MBHA resin) using 3a, 3b, and 3c appropriately and by following repetitive cycles of deprotection, neutralization, and coupling. They were cleaved from the solid support using TFA-TFMSA, purified by RP-HPLC, and characterized by MALDI-TOF mass spectrometric analysis. The known r<sub>8</sub>\_carbamate\_CF<sup>15</sup> (VI) and unlabeled r<sub>8</sub>\_carbamate\_Phe (VII) were also synthesized for comparison.

The oligocarbamates displayed a higher retention time on reversed-phase HPLC columns than the oligoamide (Supporting Information, Figure S22), demonstrating that the carbamate linkage indeed endowed the oligomers with increased hydrophobicity.

Further, partitioning experiments in model octanol–water system were performed to estimate the affinity of the oligomers for the lipid membrane.<sup>17</sup> The partitioning of the amide (I) and oligocarbamates (II and III) was monitored using CF-labeled oligomers. The oligomers were highly water-soluble and remained completely in the aqueous phase. Upon addition of sodium laurate, complete migration of amide I and carbamate II into the octanol phase was observed, whereas carbamate III was found in aqueous as well as octanol phases. The observation is indicative of the fact that the linker length indeed affects an oligomer's affinity for water as well as lipid and consequently its amphipathic nature. This partitioning could be monitored visually by the naked eye and is shown in Figure 2.

CD spectroscopic studies were then carried out to study the presence of secondary structures in these oligomers (Figure 3). The oligoamide I exhibited a significant CD pattern with prominent signals around 200 and 230 nm, indicating a structured backbone, whereas no CD pattern emerged for the oligocarbamates II and III, indicating random backbone conformations. This is in tune with the literature reports

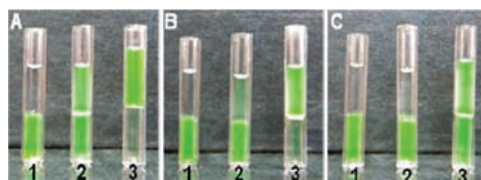


Figure 2. Partitioning of oligomers I (A), II (B), and III (C) in water–octanol without added sodium laurate (1) and with 3.0 (2) and 6.0 equiv (3) of sodium laurate/guanidinium group.

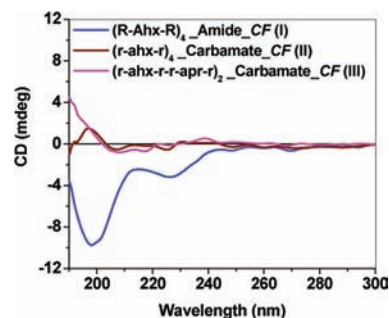


Figure 3. CD spectra of the oligoamide I and oligocarbamates II and III (10  $\mu\text{M}$ ) in water.

where replacement of a relatively rigid amide bond by the more flexible carbamate led to a loss of secondary structure.<sup>16</sup>

Thus, as per the design expectations, the oligocarbamates II and III were shown to be amphipathic in nature, similar to the oligoamide I, but less structured. It would be interesting to see if these attributes could prove to be advantageous in the case of the oligocarbamates, enabling them to easily adopt a conformation suited for membrane interactions and cellular uptake as envisaged. The oligocarbamates, endowed with better amphipathic, unstructured backbones and eight guanidine functionalities, were evaluated in this study to gauge their ability to enter cells in comparison with the control oligoamides. CF-labeled oligomers I–III and VI were used in the cellular uptake experiments. Oligomers IV, V, and VII were used for cargo delivery, in which Phe replaces the CF-tag in I, II, and VI, respectively.

Cellular uptake was determined by fluorescence-activated cell sorting (FACS) analysis in CHO-K1 cells after incubation at 37 °C for 1 h at 5  $\mu\text{M}$  concentration. CF itself did not enter cells in this assay. The uptake at 5  $\mu\text{M}$  of I and II is depicted in Figure 4. The oligomer II showed excellent uptake in nearly 100% of cells, compared to the 70% of cells showing uptake of control oligomer I. The mean fluorescence intensity for oligomer II was also about 9 times greater than that for the control oligoamide I. The uptake of II was also better than for the known r<sub>8</sub>-carbamate<sup>15</sup> VI. An additional experiment with mild acid wash, known to effectively quench cell membrane-bound fluorescence,<sup>18</sup> was carried out to ensure that only the internalized fluorescence was assayed. The relative results of cellular uptake did not show any change (data not shown); however, high cellular toxicity was observed due to the acid wash.

All energy-dependent pathways such as endocytosis are known to be inhibited at low temperatures and pre-treatment of cells with sodium azide.<sup>9</sup> To study the effect of temperature, the cellular uptake of the oligomers I, II (Figure 4), and VI was compared at 4 and 37 °C using the same protocols as above. Surprisingly, the oligocarbamate II was taken up by almost

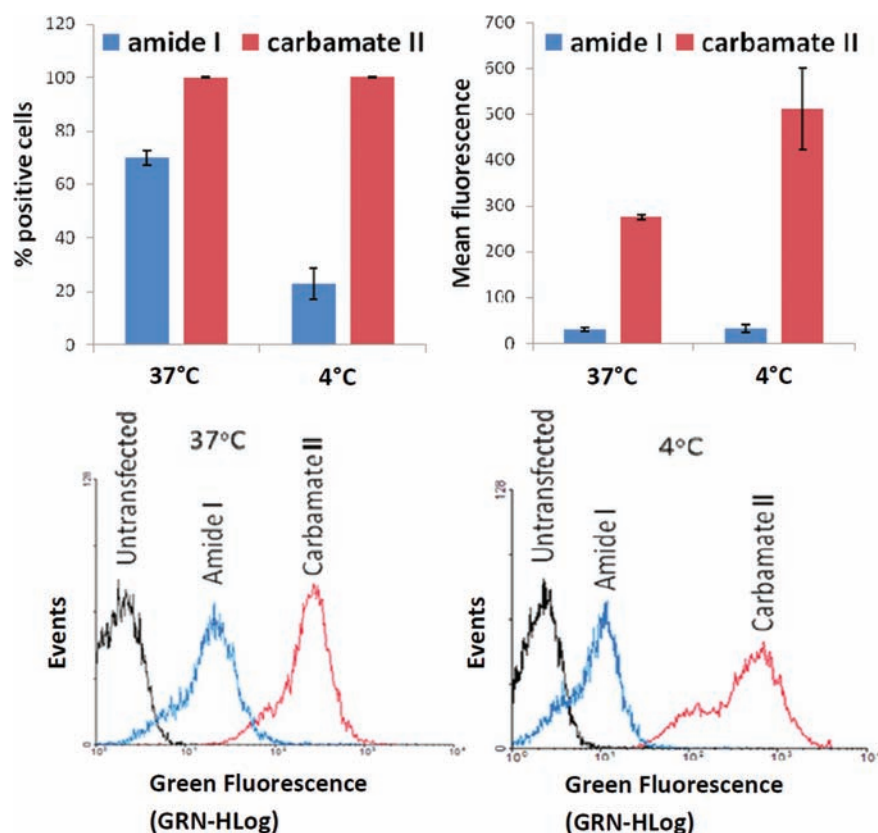


**Figure 4.** FACS data of uptake in CHO-K1 cells at 37 and 4 °C.

100% of cells at 4 °C, whereas amide I was taken up in only about 20% of cells. The ratio of mean fluorescence at 4 °C for II:I was almost 16:1. Uptake of oligomer VI was found to be adversely affected at lower temperature (Figure S28) in our studies.

Confocal microscopy studies were further undertaken in CHO-K1 cells in order to see the intracellular distribution of the synthesized oligomers. As can be seen from Figure 5, the oligomer II (at 5  $\mu$ M) exhibited strong fluorescence, with predominantly cytosolic localization. The fluorescence for the control oligoamide I was observed only at higher concentration (10  $\mu$ M) and was found in cytosol as well as near/within the

nucleus. The observed uptake of oligomer III was similar to that of oligomer II (Figure S25). The entry of the oligomer II at 4 °C was also checked by confocal microscopy. The majority of the cells showed significant uptake of the oligomer (Figure S24), confirming the energy-independent entry pathway, as indicated by the FACS analysis. Cell uptake studied by confocal microscopy after pretreating the cells with sodium azide indicated no apparent inhibition (Figure S27) of uptake and also showed the residence of oligocarbamate II mainly in the cytoplasm. These experiments clearly indicate the high efficiency of oligomer II compared to the control oligomers I and VI to enter cells by energy-independent mechanisms, most likely by direct translocation into cytoplasm, thereby reducing endosomal entrapment. Additional cell uptake experiments were then undertaken in HeLa cells using oligocarbamate II along with the control oligoamide I. As in the case of CHO-K1 cells, very high uptake localized in the cytoplasm was observed also in HeLa cells for the oligocarbamate II as compared to oligoamide I (Figures S36 and S37).

The cytotoxicity of the synthesized oligomers in CHO-K1 cells was assessed using the Cell Titer-Glo Luminescent Cell Viability Assay system (Figure S29). The oligocarbamates II and III showed viability/toxicity comparable with that of the control oligomer I at both concentrations studied and at extended time. To assess the potential applicability of oligocarbamates II, III, and VI, experiments in comparison with oligomer I in the presence of serum were also performed. The uptake of oligocarbamates was again found to be better than that of the oligoamide (Figure S30). To test the applicability of the oligocarbamates in delivering cargo molecules in biologically active form, we carried out pMIR-Report plasmid DNA transfection in CHO-K1 cells. The

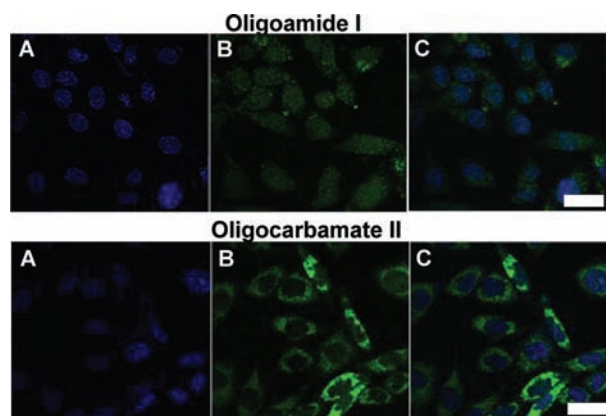


**Figure 5.** Confocal microscopy images of CHO-K1 cells after 4 h incubation at 37 °C with the oligoamide I (10  $\mu$ M) and oligocarbamate II (5  $\mu$ M). (A) Staining with nuclear stain, Hoechst 33342. (B) Fluorescence image. (C) Merged images. Scale bar: 20  $\mu$ m.



oligocarbamate V (unlabeled counterpart of oligocarbamate II was chosen to avoid any interference of the CF label), after complexation with plasmid DNA (Figure S34) and transfection, exhibited efficient expression of the reporter gene (Figure 6)

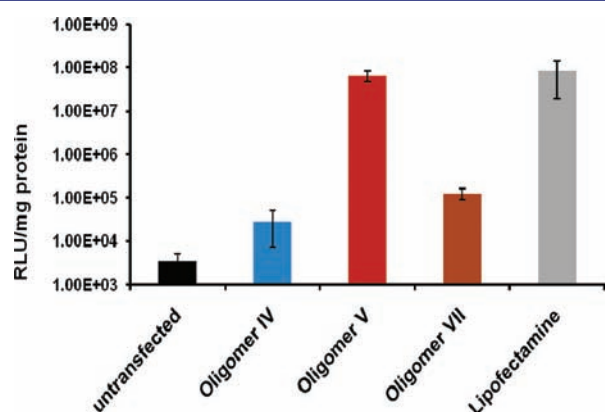


**Figure 6.** Transfection of pMIR-Report luciferase in CHO-K1 cells with unlabeled oligomers IV, V, and VII.

better than that of oligoamide IV, without using chloroquine as endosomolytic reagent,<sup>19</sup> and comparable to that of Lipofectamine2000 (Figure S35). Additionally, oligomer V–DNA complexes demonstrated much better cell viability than Lipofectamine2000. In another experiment, oligocarbamate II was found to be more efficient than I in mediating cellular entry of a covalently conjugated potential therapeutic peptide<sup>20</sup> (conjugates B and A respectively in Table S1 and Figure S32). Further, labeled siRNA (siGLO) was found to be efficiently internalized in CHO-K1 cells when complexed to oligocarbamate V, as determined by FACS analysis (Figure S33).

In conclusion, newly synthesized oligocarbamates containing the (r-x-r) motif with spaced guanidine groups were shown to be effective in cellular entry, even under conditions that inhibit endocytotic pathways. It appears that, in addition to other energy-dependent pathways, at least one pathway such as direct translocation could be at work as the major mode of transport in this case. The oligocarbamate is able to deliver a large cargo such as plasmid DNA with high reporter gene expression, without the addition of chloroquine as required for similar experiments with (R-Ahx-R)<sub>4</sub> amide.<sup>19</sup> Further, the oligocarbamates also allow efficient cellular entry of covalently conjugated peptides and siRNA in the complexed form. The strong cellular entry of the designed oligocarbamates should be extremely attractive for their further development as cellular transporters for small molecules, oligopeptides, and oligonucleotides for therapeutic applications.

## ■ ASSOCIATED CONTENT

### Supporting Information

NMR and mass spectra of 2a and 3a–c; HPLC chromatograms and MALDI-TOF spectra of oligomers; further confocal microscopy images, FACS analysis, cell viability assay, and cargo delivery data in CHO-K1 cells; FACS analysis, confocal microscopy images, and cell viability assay in HeLa cells; DNA complexation studies by gel mobility shift assay of pDNA with oligomers IV and V and cell viability assay of the complexes in CHO-K1 cells. This material is available free of charge via the Internet at <http://pubs.acs.org>.

## ■ AUTHOR INFORMATION

### Corresponding Author

va.kumar@ncl.res.in; mganguli@igib.res.in

### Author Contributions

<sup>§</sup>K.M.P. and R.J.N. contributed equally.

### Notes

The authors declare no competing financial interest.

## ■ ACKNOWLEDGMENTS

CSIR-New Delhi is acknowledged for a research grant (NWP0036A) to V.A.K.; NCL-IGIB Joint Research Initiative for funding; CSIR-New Delhi for Research Fellowships to K.M.P. and Rajpal; DBT-New Delhi for Research Fellowship to R.J.N.; and Manika Vij (IGIB) for help with some FACS experiments.

## ■ REFERENCES

- (1) Schwarze, P. M.; Dowdy, S. F. *Trends Pharmacol. Sci.* **2000**, *21*, 45.
- (2) Derossi, D.; Chassaing, G.; Prochiantz, A. *Trends Cell Biol.* **1998**, *8*, 84.
- (3) Derossi, D.; Joliot, A. H.; Chassaing, G.; Prochiantz, A. *J. Biol. Chem.* **1994**, *269*, 10444.
- (4) Mitchell, D. J.; Kim, D. T.; Steinman, L.; Fathman, C. G.; Rothbard, J. B. *J. Pept. Res.* **2000**, *56*, 318.
- (5) Naik, R. J.; Chandra, P.; Mann, A.; Ganguli, M. *J. Biol. Chem.* **2011**, *286*, 18982.
- (6) Rothbard, J. B.; Kreider, E.; VanDeusen, C. L.; Wright, L.; Wylie, B. L.; Wender, P. A. *J. Med. Chem.* **2002**, *45*, 3612.
- (7) Abes, R.; Moulton, H. M.; Clair, P.; Yang, S.-T.; Abes, S.; Melikov, K.; Prevot, P.; Youngblood, D. S.; Iversen, P. L.; Chernomordik, L. V.; Lebleu, B. *Nucleic Acids Res.* **2008**, *36*, 6343.
- (8) Jearawiriyapaisarn, N.; Moulton, H. M.; Buckley, B.; Roberts, J.; Sazani, P.; Fucharoen, S.; Iversen, P. L.; Kole, R. *Mol. Ther.* **2008**, *16*, 1624.
- (9) (a) Madani, F.; Lindberg, S.; Langel, Ü.; Futaki, S.; Graslund, A. *J. Biophys.* **2011**, *1*. (b) Richard, J. P.; Melikov, K.; Vives, E.; Verbeure, C. R. B.; Gait, M. J.; Chernomordik, L. V.; Lebleu, B. *J. Biol. Chem.* **2003**, *278*, 585.
- (10) Youngblood, D. S.; Hatlevig, S. A.; Hassinger, J. N.; Iversen, P. L.; Moulton, H. M. *Bioconjugate Chem.* **2007**, *18*, 50.
- (11) Wu, R. P.; Youngblood, D. S.; Hassinger, J. N.; Lovejoy, C. E.; Nelson, M. H.; Iversen, P. L.; Moulton, H. M. *Nucleic Acids Res.* **2007**, *35*, 5182.
- (12) Schröder, T.; Niemeier, N.; Afonin, S.; Ulrich, A. S.; Krug, H. F.; Bräse, S. *J. Med. Chem.* **2008**, *51*, 376.
- (13) Tamilarasu, N.; Huq, I.; Rana, T. M. *Bioorg. Med. Chem. Lett.* **2001**, *11*, 505.
- (14) Cooley, C. B.; Trantow, B. M.; Nederberg, F.; Kiesewetter, M. K.; Hedrick, J. L.; Waymouth, R. M.; Wender, P. A. *J. Am. Chem. Soc.* **2009**, *131*, 16401.
- (15) Wender, P. A.; Rothbard, J. B.; Jessop, T. C.; Kreider, E. L.; Wylie, B. L. *J. Am. Chem. Soc.* **2002**, *124*, 13382.
- (16) Lee, K. H.; Oh, J. E. *Bioorg. Med. Chem.* **2000**, *8*, 833.
- (17) Hawker, D. W.; Connell, D. W. *Environ. Sci. Technol.* **1989**, *23*, 961.
- (18) Chambers, J. D.; Simon, S. I.; Berger, E. M.; Sklar, L. A.; Arfors, K. E. *J. Leukoc. Biol.* **1993**, *53*, 462.
- (19) Lehto, T.; Abes, R.; Oskolkov, N.; Suhorutšenko, J.; Copolovici, D.-M.; Mäger, I.; Viola, J. R.; Simonson, O. E.; Ezzat, K.; Guterstam, P.; Eriste, E.; Smith, C. I. E.; Lebleu, B.; El Andaloussi, S.; Langel, Ü. *J. Controlled Release* **2010**, *141*, 42.
- (20) Lu, R.; Jia, J.; Bao, L.; Fu, Z.; Li, G.; Wang, S.; Wang, Z.; Jin, M.; Gao, W.; Yao, Z. *Cancer Chemother. Pharmacol.* **2006**, *57*, 248.